Applied Energy 250 (2019) 109–117

Contents lists available at ScienceDirect

Applied Energy

journal homepage: www.elsevier.com/locate/apenergy

Identification of electrical parameters for three-diode photovoltaic model using analytical and sunflower optimization algorithm

Mohammed H. Qais[a], Hany M. Hasanien[b,*], Saad Alghuwainem[a]

[a] Electrical Engineering Department, Faculty of Engineering, King Saud University, Riyadh 11421, Saudi Arabia
[b] Electrical Power and Machines Department, Faculty of Engineering, Ain Shams University, Cairo 11517, Egypt

HIGHLIGHTS

- A novel application of SFO algorithm to extract PV model parameters is presented.
- Three-diode PV model is used in this paper.
- Parameters of SFO-TDPV model are compared with other optimization based models.
- The SFO-TDPV model is verified by comparing its results with measured data.
- The error among these results records a value less than 0.5%.

ARTICLE INFO

Keywords:
Photovoltaic modeling
Solar energy
Sunflower optimization algorithm
Three-diode model

ABSTRACT

This article proposes an accurate and straightforward method for modeling and simulation of photovoltaic (PV) modules. The main target is to find the nine-parameter of a three-diode (TD) model based on the datasheet parameters, which are given by all commercial PV modules. The objective function is formulated based on short circuit, open circuit, power derivative, and maximum power equations. Two parameters (parallel resistance and photo-generated current) are calculated analytically and rest parameters are optimally designed using the sunflower optimization (SFO) algorithm. The presented method is applied to model three types of commercial PV modules (multicrystal KC200GT, poly-crystalline MSX-60, and mono-crystalline CS6K-280M). The optimal nine-parameters obtained in this paper are paralleled with that attained by other approaches. In order to assess the efficiency of the offered approach, *I-V* and *P-V* characteristics are validated with measured data under various temperatures and solar irradiations. The error among these results records a value less than 0.5%. Therefore, the simulation results indicate an excellent agreement with the measured data. This proposed approach can be utilized to model any marketable PV module based on given datasheet parameters only.

1. Introduction

Renewable energy systems have received much interest worldwide because of many reasons such as fossil fuel cost and its depletion probability, political and environmental concerns [1–4]. According to the published report of renewable energy at the end of 2018 by REN21, a robust increase in the renewable energy area is revealed, where solar photovoltaic (PV) capacity investments in 2017 were 99 GW representing almost twice those of wind energy (52 GW), due to the large growth of PV installations in China [5]. Generally, PV market extension is due mainly to, (1) an increase in competition of solar PV manufacturers [6]; (2) rising request for electricity in developing countries [7]; (3) responsibilities of reducing carbon dioxide releases [8,9]; and (4) price reduction of PV modules [10]. PV modules are used in domestic applications, rural electrification, and space shuffle applications. Moreover, there are large grid-connected PV power plants installed around the world such as Tengger Desert Solar Park in China which has a peak output power of 1547 MW [11]. These grid-connected PV systems require an excessive study and accurate modeling of PVs to expect the performance of physical PV modules under several environmental conditions, the maximum power extraction, the behavior of shaded PVs, and abnormal operations of the grid such as low voltage faults. The electrical modeling of PVs should represent all losses inside PV cells and the current-voltage (*I-V*) features of PV cells [12]. The ideal modeling of PV cells is considered as a photo-generated current supply (I_{ph}), which proportionate to the solar irradiation (G) falling on it. However, real

* Corresponding author.
E-mail addresses: mqais@ksu.edu.sa (M.H. Qais), hanyhasanien@ieee.org (H.M. Hasanien), saadalgh@ksu.edu.sa (S. Alghuwainem).

https://doi.org/10.1016/j.apenergy.2019.05.013
Received 25 January 2019; Received in revised form 12 April 2019; Accepted 1 May 2019
Available online 09 May 2019
0306-2619/ © 2019 Elsevier Ltd. All rights reserved.

Nomenclature

AM	air mas
E_g	band gap energy (eV)
G	solar irradiation (W/m^2)
I	the produced current of PV array (A)
I_{oi}	reverse saturation current of diode i (A)
I_m	maximum output current of PV array (A)
I_{ph}	photo-generated current (A)
I_{sc}	short circuit output current of PV module (A)
k_B	Boltzmann's constant (1.38065e-23 J/K)
n_i	ideality factor of diode i
N_s	number of series cells in PV module
P	output power of PV module (W)
P_m	maximum output power of the PV module (W)
q	electron charge (1.6022e-19C)
R_s	series resistance (Ω)
R_p	parallel resistance (Ω)
T	cell temperature (K)
V	output voltage of PV module (V)
V_m	maximum output voltage of the PV module (V)
V_{oc}	open circuit output voltage of PV module (V)
V_t	thermal voltage (V)
P_S	sun power (W)

Abbreviations

SFO	sunflower optimization algorithm
PV	photovoltaic
SD	single-diode
DD	double-diode
TD	three-diode

photo-generated current differs due to the optical and electrical losses inside the positive-negative (p-n) junction of the PV cell, which lead to the lone diode model of the PV cell. The single-diode (SD) model represents the diffusion and recombination in the quasi-neutral regions of emitter and majority zones. For obtaining more precise modeling of the PV cell losses, the double-diode (DD) model is utilized in representing recombination in the space charge region (SCR) in addition to SD losses. Lately, the three-diode (TD) model appeared to represent previous losses and recombination in defect regions and grain boundary [13]. The number of SD parameters are five parameters which are, photo-generated current (I_{ph}), series resistance which represents contact and wiring losses (R_s), parallel resistance which represents leakage current losses inside the p-n junction (R_p) [14], and diode parameters (ideality factor (n), and reverse saturation current (I_o)). There are seven parameters for the DD model (five parameters of SD + two parameters of the second diode). Finally, there are nine parameters for TD model (seven parameters of DD + two parameters of the third diode).

In a literature review, SD and DD models are the most studied and modeled by the researchers due to their low number of parameters and can be attained by analytical methods, iterative methods, numerical, or meta-heuristic optimization algorithms. Analytical methods can extract parameters from datasheet elements (I_m, V_m, P_m, V_{oc}, and I_{sc}) at standard test conditions (STC)(G is 1000 W/m^2, T is 25 °C, and AM is 1.5). These methods don't require any measurements but some approximations are inserted to reduce the number of parameters. Some researchers proposed analytical methods including approximations such as the initial value of R_p [15], initial value of I_o [16], proposed relation between n and V_{oc} [17], Lambert function method [18,19], neglecting R_p [20,21], using specified values of R_s and R_p (0.33 Ω and 135 Ω) [22], compound of calculations and curve fitting [23], considering the effect of solar radiation and temperature [24,25], and the linear least-squares method [26]. However, analytical methods for DD models require more approximations and combined analytical and iterative methods that are used in [27–29]. Iterative methods such as Gauss-Seidel method [30] and Newton-Raphson with maximum likelihood estimator are implemented in [31]. The demerit of iterative methods is the given initial values, which can lead to locally optimal solutions. Other researchers used the measured *I-V* features to start parameters extraction of the SD model using reduced forms [32,33].

On the other hand, meta-heuristic algorithms are exploited to get five-parameters of SD model and seven-parameters of DD model by minimizing proposed cost functions. Some researchers used root mean square error (RMSE) as a cost function, which requires calculation of the variance between measured and estimated current values. The researchers applied different meta-heuristic algorithms to minimize the RMSE, for example, particle swarm algorithm [34], hybrid artificial bee colony and trust-region-reflective (TRR) algorithm [35], whale optimization algorithm (WOA) [36–39], hybrid firefly algorithm and pattern search algorithm [40], water cycle algorithm (WCA) [41], salp swarm algorithm (SSA) [42], Jaya algorithm [43], harmony search algorithm (HSA) [44], Flower pollination algorithm (FPA) [45], Multiple-learning back-tracking search algorithm (MLBSA) [46], and hybrid teaching-learning and artificial bee colony algorithm (TL-ABC) [47]. Other researchers proposed different cost functions based on datasheet values and then applied meta-heuristic algorithms to solve the aforementioned problem such as differential evolution (DE) [48–51], shuffled frog leaping algorithm [52], and bacterial foraging algorithm [53].

Recently, the TD model with nine-parameters has been studied and modeled to exhibit most of the losses inside PV cells. The analytical modeling of the TD model is difficult because of the large number of parameters and a low number of nonlinear equations. Meta-heuristic algorithms are utilized to reduce the RMSE to find the nine-parameters of TD model. These meta-heuristics are PSO [13], moth flame algorithm [54], and WOA [36,39]. Many algorithms emerged recently and can be applied to attain the nine-parameters of TD model such as sunflower optimization algorithm (SFO) [55]. Actually, the need to apply the SFO in this study comes from welcoming new meta-heuristic algorithm applications, where one algorithm can solve an optimization problem and in the meantime fails to solve another one and this is based on No free lunch theorem. Therefore, the applications of new meta-heuristic algorithms are appreciated and welcomed.

The SFO is designed by Gomes and others [55] in 2018. It is a new meta-heuristic algorithm that stimulated by the movement of sunflowers towards the sunlight [56]. In addition to its movement, the pollination between random adjacent sunflowers is modeled. Furthermore, the SFO is stimulated by the inverse-square law of radiation intensity, where the amount of heat is proportional to the squared distance between sunflowers and the sun. The SFO is tested using benchmark functions and applied to detect the mechanical destruction in laminated composite plates. Due to the early emerging of SFO and based on the literature survey, the SFO is not applied to solar cell parameters extraction.

The main contributions of this paper are summarized as follows:

- Reducing nine-parameters of the TD model into seven-parameters, where R_p and I_{ph} are calculated analytically.
- A novel cost function is offered to find nine-parameters of the TD model of PV cell based on datasheet parameters.
- A novel application of the SFO algorithm is exhibited to minimize the proposed cost function.
- Three types of PV cells are modeled in this paper (Multi-crystal KC200GT (200 W), poly-crystalline MSX-60 (60 W), and mono-crystalline CS6K-280M (280 W)).

- Comparing the *I-V* and *P-V* features that are attained by the proposed approach with measured values and comparing the absolute current error of the offered method with other methods.

2. Mathematical modeling of PV module

2.1. TD model

The PV array is designed as a current source that is paralleled with three diodes and resistance then connected in series with a small resistance, as displayed in Fig. 1 [13,14].

According to the current divider rule, the current source is divided into parallel diodes and resistance then the produced current of the PV module is written as follows:

$$I = I_{ph} - \sum_{i=1}^{d} I_{Di} - \frac{V_D}{R_p} \tag{1}$$

where d is the number of diodes ($d = 3$), V_D is the voltage across diodes, and I_{Di} is the current in diode i which is expressed as follows:

$$I_{Di} = I_{0i}(e^{\frac{V_D}{n_i V_t}} - 1) \tag{2}$$

$$V_D = V + IR_s$$

$$V_t = \frac{k_B T}{q}$$

Then by sub. (2) in (1) results in

$$I = I_{ph} - \sum_{i=1}^{d} I_{0i}(e^{\frac{V+IR_s}{n_i V_t}} - 1) - \frac{V + IR_s}{R_p} \tag{3}$$

For short circuit case, the output voltage $V = 0$ and $I = I_{sc}$, and the current equation is expressed as follows:

$$I_{sc} = I_{ph} - \sum_{i=1}^{d} I_{0i}(e^{\frac{I_{sc}R_s}{n_i V_t}} - 1) - \frac{I_{sc}R_s}{R_p} \tag{4}$$

For open-circuit case, the output current is $I = 0$ and $V = V_{oc}$ and the voltage equation is written as follows:

$$0 = I_{ph} - \sum_{i=1}^{d} I_{0i}(e^{\frac{V_{oc}}{n_i V_t}} - 1) - \frac{V_{oc}}{R_p} \tag{5}$$

By subtracting (5) from (4) then

$$I_{sc} + \frac{I_{sc}R_s}{R_p} = \sum_{i=1}^{d} I_{0i}(e^{\frac{V_{oc}}{n_i V_t}} - e^{\frac{I_{sc}R_s}{n_i V_t}}) + \frac{V_{oc}}{R_p}$$

$$I_{sc} = \frac{R_p}{R_p + R_s}\left[\sum_{i=1}^{d}\left\{I_{0i}(e^{\frac{V_{oc}}{n_i V_t}} - e^{\frac{I_{sc}R_s}{n_i V_t}})\right\} + \frac{V_{oc}}{R_p}\right]$$

$$Z_i = I_{0i}(e^{\frac{V_{oc}}{n_i V_t}} - e^{\frac{I_{sc}R_s}{n_i V_t}})$$

Then the short circuit current I_{sc} can be expressed as follows:

$$I_{sc} = \frac{R_p}{R_p + R_s}\left[\sum_{i=1}^{d} Z_i + \frac{V_{oc}}{R_p}\right] \tag{6}$$

The power derivative (slope) is zero at the maximum power point as follows

$$P = V \times I \text{ then } \frac{dP}{dV} = I + V\frac{dI}{dV} = 0$$

$$\frac{dI}{dV} = \frac{-I_m}{V_m} \tag{7}$$

Then the derivative of (3) is expressed as follows:

$$\frac{dI}{dV} = 0 - \sum_{i=1}^{d} I_{0i}\frac{d}{dV}\left(e^{\frac{V+IR_s}{n_i V_t}}\right) - \frac{1}{R_p} - \frac{R_s}{R_p}\frac{dI}{dV}$$

$$\frac{dI}{dV} + \frac{R_s}{R_p}\frac{dI}{dV} = -\sum_{i=1}^{d} I_{0i}\frac{d}{dV}\left(e^{\frac{V+IR_s}{n_i V_t}}\right) - \frac{1}{R_p}$$

$$(\frac{Rp + Rs}{Rp})(\frac{dI}{dV}) = -\sum_{i=1}^{d} I_{0i}(\frac{1 + \frac{dI}{dV}R_s}{n_i V_t})e^{\frac{V+IR_s}{n_i V_t}} - \frac{1}{R_p}$$

$$(\frac{Rp + Rs}{Rp})(\frac{I_m}{V_m}) = \sum_{i=1}^{d} I_{0i}(\frac{1 - \frac{I_m}{V_m}R_s}{n_i V_t})e^{\frac{V_m + I_m R_s}{n_i V_t}} + \frac{1}{R_p}$$

$$Y_i = I_{0i}(\frac{V_m - I_m R_s}{n_i V_t})e^{\frac{V_m + I_m R_s}{n_i V_t}}$$

Then the maximum current I_m can be expressed as follows:

$$I_m = \frac{R_p}{R_p + R_s}\left[\sum_{i=1}^{d} Y_i + \frac{V_m}{R_p}\right] \tag{8}$$

By dividing (8) and (6), R_p is expressed as follows:

$$R_p = \frac{V_{oc}I_m - V_m I_{sc}}{\sum_{i=1}^{d}\{I_{sc}Y_i - I_m Z_i\}} \text{ where } R_p > 0 \tag{9}$$

From (5), I_{ph} is expressed as follows:

$$I_{ph} = \frac{V_{oc}}{R_p} + \sum_{i=1}^{d} I_{0i}(e^{\frac{V_{oc}}{n_i V_t}} - 1) \tag{10}$$

The maximum power P_m is expressed as follows:

$$P_m = V_m \times I_m = V_m \times \left(I_{ph} - \sum_{i=1}^{d} I_{0i}(e^{\frac{V_m + I_m R_s}{n_i V_t}} - 1) - \frac{V_m + I_m R_s}{R_p}\right) \tag{11}$$

2.2. SFO algorithm

The SFO is a new meta-heuristic algorithm which is stimulated by the moving of sunflowers towards the sunlight by considering the pollination between adjacent sunflowers. Also, the SFO is stimulated by the inverse square law radiation [55]. If the distance between sunflowers and sun increases, the radiation intensity will decrease and vice versa according to (12).

$$G = \frac{P_S}{4\pi r^2} \tag{12}$$

where G is the solar radiation intensity, P_S is the sun power, and r is the distance between sunflower and sun. The direction s_i of plants towards the sun is expressed as:

$$\vec{s_i} = \frac{X^* - X_i}{\|X^* - X_i\|} \quad i = 1, 2, 3, \ldots n_p \tag{13}$$

where X^* and X_i are the best and current positions of sunflowers directions towards the sun, n_p is the number of sunflowers, and $\|\ \|$ is the norm operator.

The step of sunflowers in the direction of the sun is expressed as:

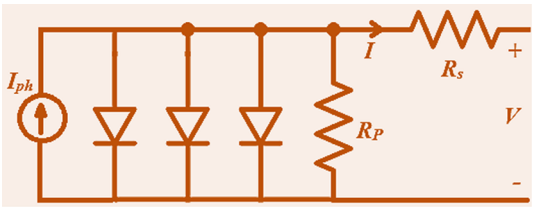

Fig. 1. three-diode model of PV Module [13].

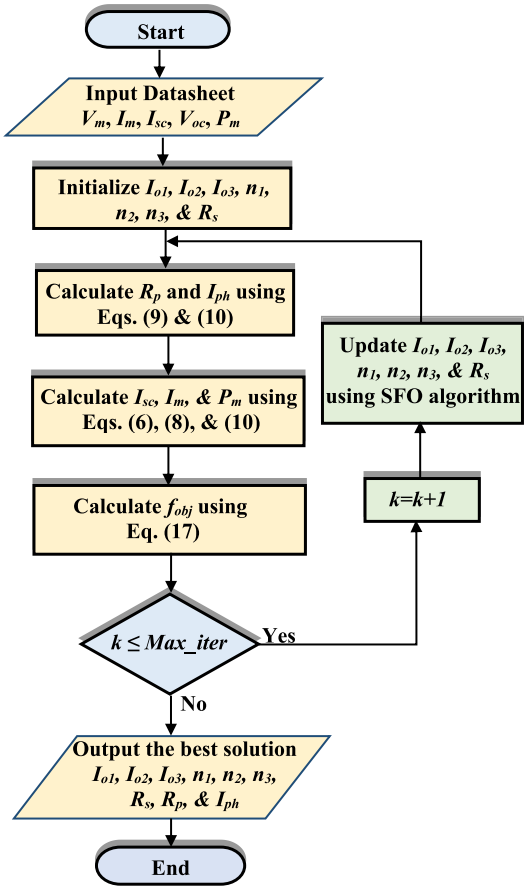

Fig. 2. Flowchart of proposed SFO-based nine-parameter identification.

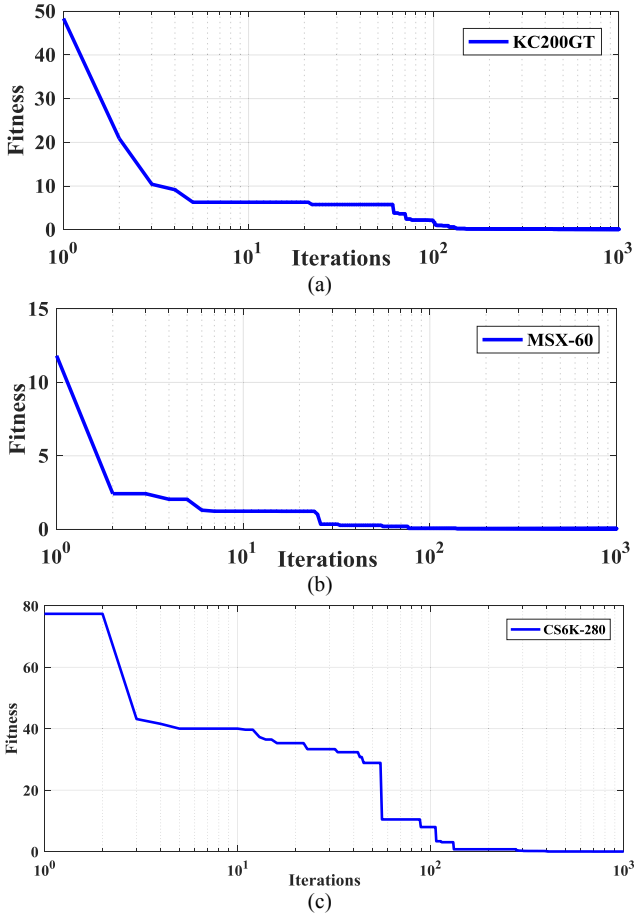

Fig. 3. Convergence curves of: a) KC200GT; b) MSX-60; c) CS6k-280M.

Table 1
Datasheet of three marketable PV modules at STC.

Company	Kyocera [57]	Solarex [58]	Canadian Solar [59]
Model	KC200GT	MSX-60	CS6K-280M
Cell type	Multicrystal	Polycrystalline	Mono-crystalline
P_m [W]	200	60	280
V_m [V]	26.3	17.1	31.5
I_m [A]	7.61	3.5	8.89
V_{oc} [V]	32.9	21.1	38.5
I_{sc} [A]	8.21	3.8	9.43
Ns [cells]	54	36	60
Ki	0.00318 A/°C	0.065%/°C	0.053%/°C
Kv	−0.123 V/°C	−0.08 V/°C	−0.31%/°C

$$d_i = \lambda \times P_i(\|X_i + X_{i-1}\|) \times \|X_i + X_{i-1}\| \tag{14}$$

where λ is inertial displacement of sunflowers and $P_i(\|X_i + X_{i-1}\|)$ is the pollination probability where each sunflower *i* fertilizes with its adjacent *i-1* generating individuals in an arbitrary position that differs regarding the distance between the sunflowers. The maximum step of individuals is restricted as follows

$$d_{\max} = \frac{\|X_{\max} - X_{\min}\|}{2 \times N_{pop}} \tag{15}$$

where X_{max} and X_{min} are higher and lower constraints value and N_{pop} is the number of sunflowers of the whole population. The next population is updated by the following equation:

$$\bar{X}_{i+1} = \bar{X}_i + d_i \times \bar{s}_i \tag{16}$$

where X_{i+1} is the new position of sunflowers.

The pseudo code of the SFO algorithm is displayed in Algorithm 1. The algorithm starts with a random initialization of the population of sunflowers. Each generated entity is evaluated to find who is directed towards the sun, which represents the best candidate among all. Then, all the remaining entities orientate themselves, like the sunflowers, in

Table 2
Optimum parameters using SFO-based proposed method.

	KC200GT	MSX-60	CS6K-280
I_{ph} (A)	8.21213	3.80111	9.440369
R_p (Ω)	606.1219	578.3468	2.16E+04
R_s (Ω)	0.23796	0.20598	0.2
n_1	1.2481	1.282	2
n_2	1.991	1.8043	2
n_3	1.8421	1.4364	1.1913
I_{o1} (A)	4.30E−08	4.98E−08	1.00E−12
I_{o2} (A)	2.22E−10	7.24E−10	1.00E−12
I_{o3} (A)	1.35E−06	1.42E−07	7.46E−09

Table 3
Comparison of optimum parameters for KC200GT.

	GA [39]	SA [39]	WOA [39]	SFO
I_{ph}(A)	8.143	8.25	8.231	8.21213
I_{o1}(A)	1.52e−8	1.78e−8	2.692e−8	4.30E−08
I_{o2}(A)	4.58e−10	3.76e−10	4.678e−10	2.22E−10
I_{o3}(A)	1.019e−10	4.62e−10	4.927e−10	1.35E−06
n_1	1.189	1.199	1.32	1.2481
n_2	1.495	1.2	1.236	1.991
n_3	1.38	1.48	1.0216	1.8421
R_s(Ω)	0.3614	0.378	0.3421	0.23796
R_p(Ω)	311.8	327.597	341.387	606.1219

Table 4
Comparison of optimum parameters for MSX-60.

	GA	SA	WOA	SFO
I_{ph}(A)	3.801	3.792	3.756	3.80111
I_{o1}(A)	1.64e−8	1.98e−8	2.192e−8	4.98E−08
I_{o2}(A)	4.82e−10	4.76e−10	3.68e−10	7.24E−10
I_{o3}(A)	1.29e−10	2.62e−10	3.97e−10	1.42E−07
n_1	1.21	1.29	1.30	1.282
n_2	1.25	1.22	1.23	1.8043
n_3	1.30	1.28	1.03	1.4364
R_s(Ω)	0.181	0.211	0.195	0.20598
R_p(Ω)	280.22	298.59	277.37	578.3468

Table 5
Comparison of optimum parameters for CS6K-280M.

	MLE [31]	WOA	SFO
I_{ph}(A)	9.46	9.516574724	9.440369
I_{o1}(A)	10e−10	6.03528E−06	1.00E−12
I_{o2}(A)	–	3.21299E−06	1.00E−12
I_{o3}(A)	–	1E−12	7.46E−09
n_1	1.108	1.841521006	2
n_2	–	1.750541567	2
n_3	–	1.623788571	1.1913
R_s(Ω)	0.168	0.01351602	0.2
R_p(Ω)	599.99	1.50E+03	2.16E+04

the direction of the sun and change arbitrarily organized, which means that they yield random steps in a particular direction.

Algorithm 1 [55]

Initialize the search agents of sunflowers
Find the fitness function and the best position (sun)
Adjust all sunflowers in the direction of the sun as in (13)
while *(k < Max_iter)*
Compute the direction vector for every search agents
Eliminate m(%) sunflowers further away from the sun
Compute the step for every sunflower as in (14)
Best sunflowers will fertilize nearby the sun
Assess the new entities
If a new entity is a universal best, update the best position
end while
output the best positions

2.3. Proposed method

The objective function f_{obj} is the sum of absolute differences between datasheet parameters (I_{sc_dsht}, I_{m_dsht}, and P_{m_dsht}) and calculated parameters (I_{sc_cal}, I_{m_cal}, and P_{m_cal}) using Eqs. (6), (8), and (11) which can be expressed as follows:

$$f_{obj} = |I_{m\_cal} - I_{m\_dsht}| + |I_{sc\_cal} - I_{sc\_dsht}| + |P_{m\_cal} - P_{m\_dsht}| \quad (17)$$

where the parameters (I_{o1}, I_{o2}, I_{o3}, n_1, n_2, n_3, and R_s) are generated using the SFO algorithm and parameters (R_p and I_{ph}) are calculated using (9) and (10), as shown in Fig. 2. The search range of I_{oi} is

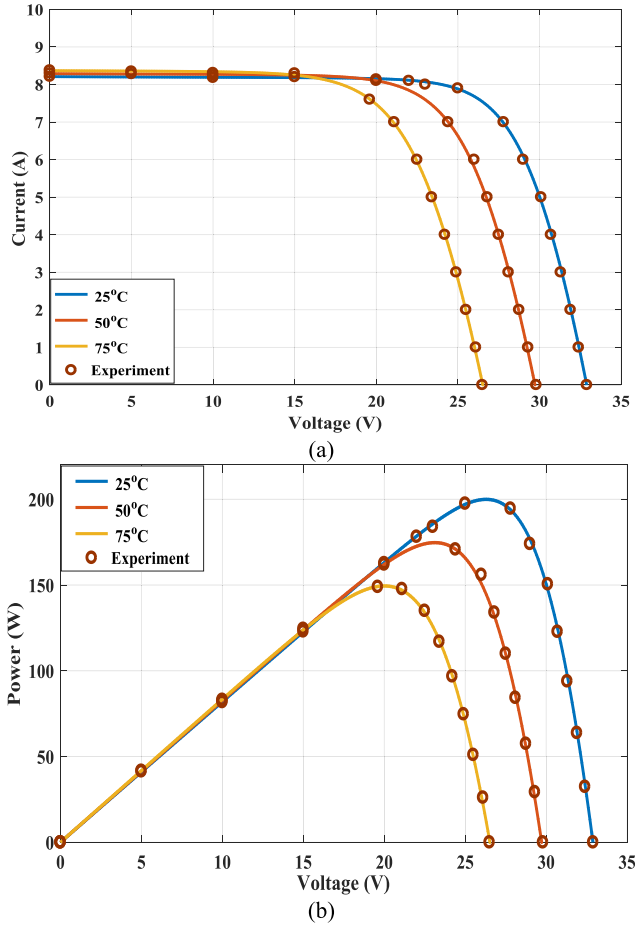

Fig. 4. Numerical results for KC200GT at different T, AM 1.5, and G = 1000 W/m^2 (a) I-V curves; (b) P-V curves.

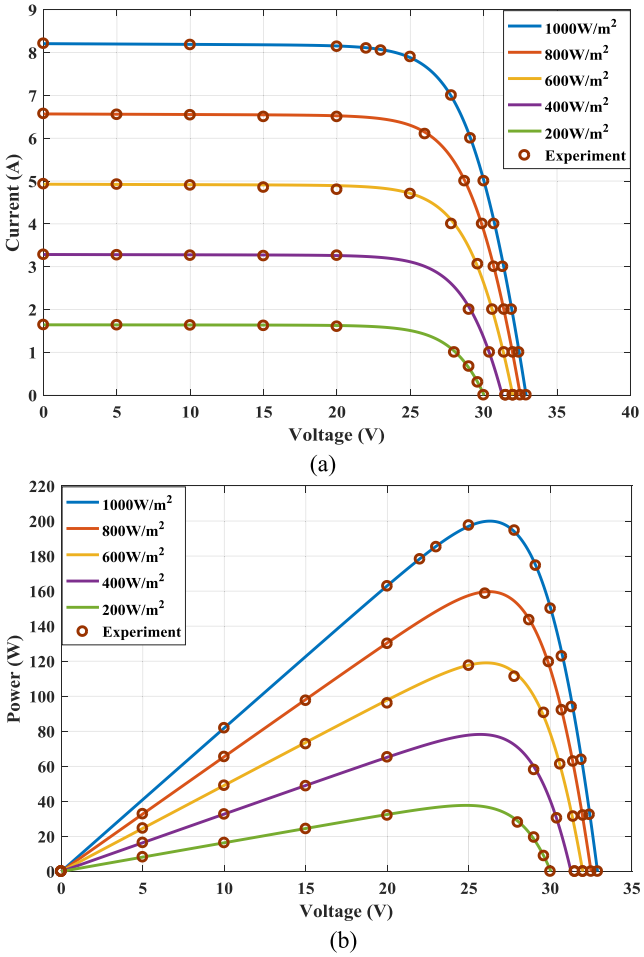

Fig. 5. Numerical results for KC200GT at different G, AM 1.5, and T = 25 °C (a) I-V curves; (b) P-V curves.

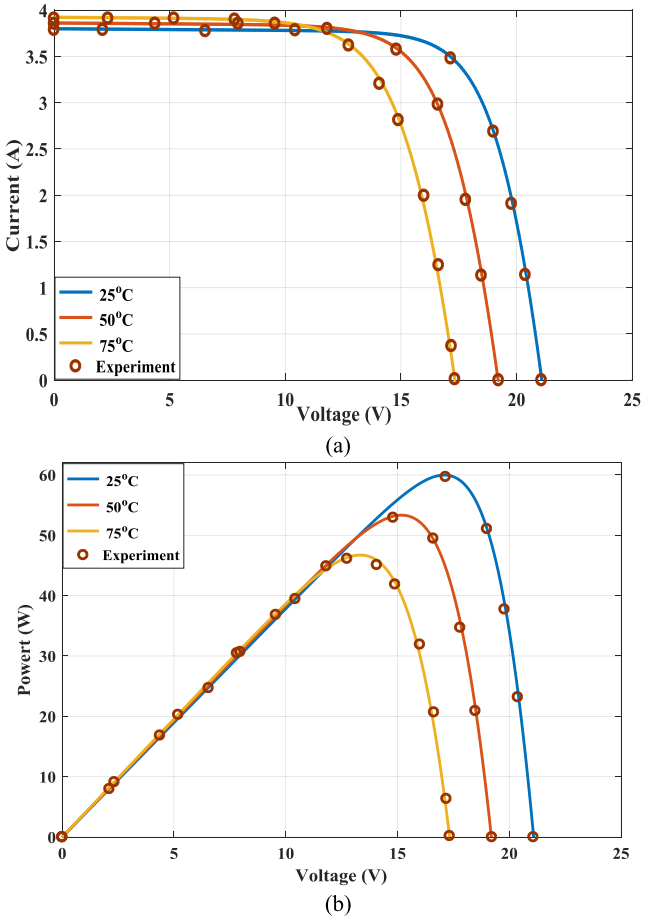

Fig. 6. Numerical results for MSX-60 at different T, *AM* 1.5, and $G = 1000\ \mathrm{W/m^2}$ (a) *I-V* curves; (b) *P-V* curves.

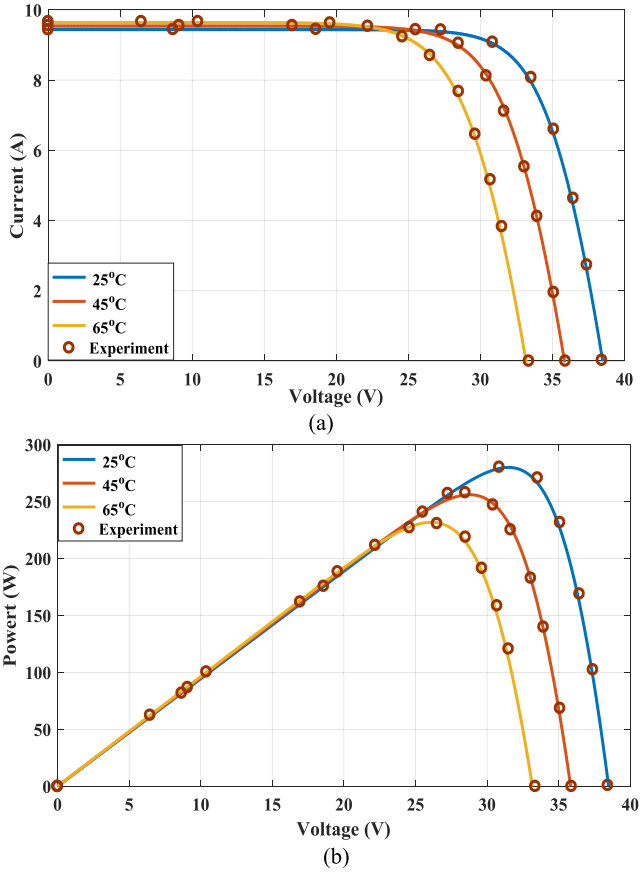

Fig. 7. Numerical results for CS6K-280M at different T, *AM* 1.5, and $G = 1000\ \mathrm{W/m^2}$ (a) *I-V* curves; (b) *P-V* curves.

[10–5,10–12], $n_i \in$ [1,2], and $R_s \in [0, 1]$. The mathematical modeling and objective functions depend on datasheet parameters which can be utilized to model any commercial PV arrays. Environmental conditions (T and G) affect parameters of PV modules as follows:

$$\begin{aligned} I_0 &= I_{0n}\left(\frac{T}{T_n}\right)^3 e^{\frac{qE_g}{nK_B}\left(\frac{1}{T_n}-\frac{1}{T}\right)} \\ E_g &= E_{gn}(1 - 0.0002677\ \Delta T) \\ R_p &= R_{pn}\frac{G_n}{G} \\ I_{ph} &= (I_{phn} + k_i \Delta T)\frac{G}{G_n} \end{aligned} \tag{18}$$

where n denotes STC conditions.

3. Numerical results and discussion

In this section, the offered method can be employed to model any marketable PV modules because it depends on datasheet parameters, not experimental data. It is validated and applied to identify nine-parameters of a TD model of three well-known marketable PV modules. These PV modules differ in the power capacity, cell type, and manufacturers (KC200GT [57], MSX-60 [58], and CS6K-280M [59]) and their electrical characteristics are indicated in Table 1. The reason for selecting these PV modules in this study is that they are famous PV module suppliers where the Canadian solar manufacturer (CS6k-280M) listed in the top 10 PV suppliers in 2017 [60]. Datasheet parameters (I_m, V_m, P_m, V_{oc}, and I_{sc}) of three marketable PV modules are recorded at STC conditions, as shown in Table 1.

The SFO algorithm is employed to minimize the objective function (17) where the number of plants is 100, the number of iteration is 1000, the probability of pollination is 5%, $\lambda = 1$, and the number of removed plants m = 10%. These optimal settings of the SFO algorithm are achieved based on the designer experience, where the trial and error method is implemented to achieve an optimal design of the SFO algorithm. In this regard, this method is the most commonly used for fine-tuned meta-heuristic algorithm settings. The convergence curves of the objective function for the TD model of KC200GT, MSX-60, and CS6K-280M PV modules are illustrated in Fig. 3 (a)-(c), respectively. These convergence curves are very smooth and terminate to a minimum fitness value that is close to zero. These optimization and simulation results are executed using MATLAB 2016b [61] on a PC that has the following specifications: Intel(R) Core(TM) i7-3770 CPU @ 3.4 GHz Processor, 16 GB RAM, 64-bit operating system. The optimum nine-parameters of the TD model of the three marketable PV modules are shown in Table 2. Furthermore, a reasonable comparison is made in order to investigate the validity of these optimum parameters of the proposed TD model. In the light of this comparison, optimal parameters of the proposed method are compared with optimal parameters that attained by genetic algorithm (GA), simulated annealing (SA), and WOA for KC200GT and MSX-60 modules, as shown in Tables 3 and 4. The optimum parameters of the TD model for CS6K-280M module are compared with the optimum parameters of the SD model using maximum likelihood estimator (MLE) [31] and TD model using the WOA as listed in Table 5. It can be realized from these results that the optimal parameter of the proposed TD model is very close to that obtained by using other meta-heuristic optimization algorithms.

In addition, the offered approach is verified by comparing its *I-V* and *P-V* curves with the experiment curves under various T and G. For KC200GT module, the proposed method is tested under *AM* 1.5, constant $G = 1000\ \mathrm{W/m^2}$ and different T (25, 50, and 75 °C) then the drawn *I-V* and *P-V* curves are validated with measured data, as shown

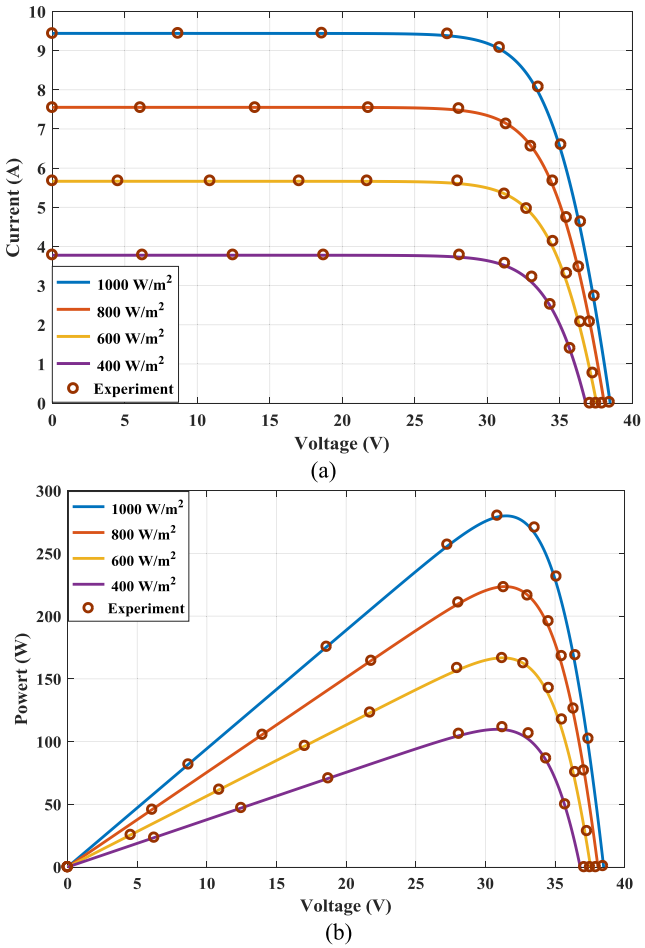

Fig. 8. Numerical results for CS6K-280M at different *G*, *AM* 1.5, and $T = 25\,^{\circ}C$, (a) *I-V* curves; (b) *P-V* curves.

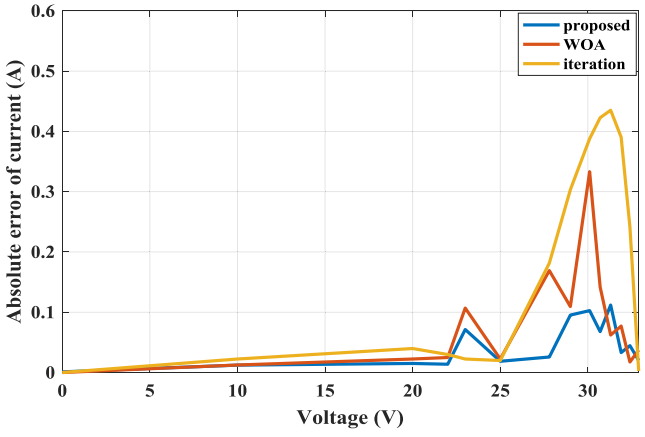

Fig. 9. Absolute error of current for KC200GT module.

in Fig. 4-(a) and (b). On the other hand, the *I-V* and *P-V* curves under constant $T = 25\,^{\circ}C$ and *G* is varying (1000, 800, 600, 400, and 200 W/m^2) are drawn as illustrated in Fig. 5-(a) and (b). *I-V* and *P-V* curves revealed the efficacy of the offered approach under various environmental conditions compared to the measured data for KC200GT module. For MSX-60 module, *I-V* and *P-V* curves of the proposed method are indicated under constant $G = 1000\,W/m^2$ and different *T* (25, 50, and 75 °C) then they are validated with measured data as demonstrated in Fig. 6-(a) and (b). For CS6K-280M module, *I-V* and *P-V* curves of the proposed method are illustrated under constant

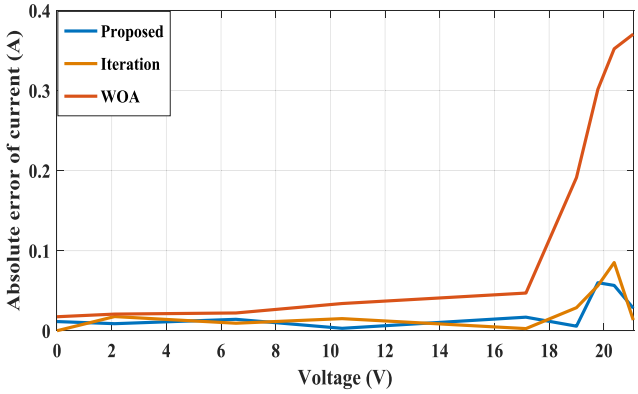

Fig. 10. Absolute error of current for MSX-60 module.

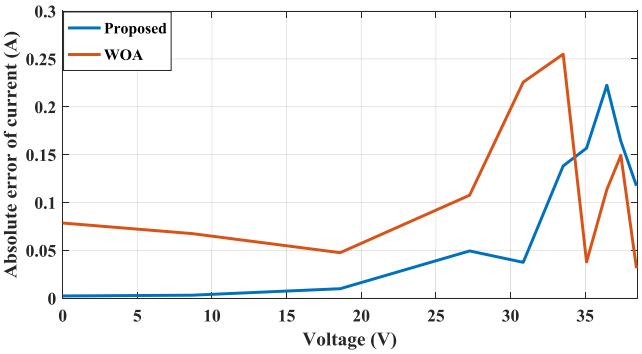

Fig. 11. Absolute error of current for CS6K-280M module.

$G = 1000\,W/m^2$ and different *T* (25, 45, and 65 °C) then they are validated with measured data as shown in Fig. 7-(a) and (b). On the other hand, *I-V* and *P-V* curves under constant $T = 25\,^{\circ}C$ and *G* is varying (1000, 800, 600, and 400 W/m^2) are demonstrated in Fig. 8-(a) and (b). All the measured data are obtained on the rooftop of a Campus building. In these tests, each PV module is loaded by a variable resistor and its nominal value is 39 Ω. This resistor can be varied within its range in steps and in each step a digital multimeter is used to record the PV current and voltage. A silicon-cell Pyranometer SP-110-SS with a calibration factor of 5 W/m^2 per mV is used to measure the solar irradiance. A high probe infrared electronic thermometer temperature gauge with an accuracy of +1 °C and its temperature range is [–32 to 550 °C] is implemented to measure the temperature.

For further verification of the offered approach, its absolute error of current (AEC) is validated with other approaches. For KC200GT module, The AEC of the offered approach is compared with the WOA [39] and the iteration method [62]. It is obvious that the proposed method offered a smaller error than that achieved by using other methods as shown in Fig. 9. For MSX-60 module, the AEC of the offered approach is less than the AEC by using both of the iteration method [62] and WOA, where the proposed method offered smaller error, as depicted in Fig. 10. The AEC for CS6K-280M is compared with the WOA as shown in Fig. 11.

4. Conclusion

The principal aim of this paper is to attain a precise PV model for any commercial PV module. In order to represent most of losses in a real PV module, a TD model is presented in this article. The nonlinear *I-V* equation of TD model has nine parameters which are identified using the incorporated analytical method and SFO algorithm. The objective function is formulated using short circuit, open circuit, a derivative of power, and maximum power equations. The SFO is applied to minimize

this function and design seven optimal parameters (I_{o1}, I_{o2}, I_{o3}, n_1, n_2, n_3, and R_s) and other parameters (R_p and I_{ph}) are calculated analytically. The presented method is applied to find the optimal TD model of three well-known marketable PV modules such as KC200GT, MSX-60, and CS6K-280M. The optimal parameters obtained are very close and competitive to that obtained by using other methods, where the proposed SFO algorithm has exhibited a minimum optimal fitness value of 1.23×10^{-12}. Moreover, the *I-V* and *P-V* curves of the offered method are validated with measured data under various working and environmental conditions and the error among these results records a value less than 0.5%. This indicates the effectiveness and robustness of the presented method for attaining an accurate TD model of the PV module. It can be concluded that theoffered approach can be applied to yield the most accurate model of any commercial PV modules. The proposed SFO algorithm may be applied to solve several engineering optimization problems in the energy sector, smart grids, and power systems.

Acknowledgement

The authors extend their gratitude to the Deanship of Scientific Research at King Saud University for funding this paper through research group No (RG-1440-049).

Appendix A

The equations of updating whales position for the WOA are written as follows [63]:

$$\begin{cases} X_{t+1} = X_{rand} - A.\ |C.\ X_{rand} - X_t| \text{ if } |A| > 1 \& r_1 < 0.5 \\ X_{t+1} = X^* - A.\ |C.\ X^* - X_t| \text{ if } |A| < 1 \& r_1 < 0.5 \\ X_{t+1} = X^* + |X^* - X_t|.\ e^{bl}.\ \cos(2\pi l) \text{ if } r_1 >= 0.5 \end{cases} \tag{19}$$

$$A = 2.\ a.\ r_2 - 2$$

$$a = 2 - 2\frac{t}{t_{\max}}$$

$$C = 2.\ r_3$$

where t is the current iteration, t_{max} is the maximum allowed number of iterations, r_1, r_2, r_3 are random numbers in the range [0, 1], X_{t+1} is a new position, X^* is the best position, and X_t is the current position.

References

[1] Qais Mohammed H, Hasanien Hany M, Alghuwainem Saad. Enhanced salp swarm algorithm: Application to variable speed wind generators. Eng Appl Artific Intel 2019;80:82–96.
[2] Hasanien Hany M. Performance improvement of photovoltaic power systems using an optimal control strategy based on whale optimization algorithm. Electr Power Syst Res 2018;157:168–76.
[3] Kalaam Rahila N, Muyeen SM, Al-Durra Ahmed, Hasanien Hany M, Al-Wahedi Khaled. Optimisation of controller parameters for grid-tied photovoltaic system at faulty network using artificial neural network-based cuckoo search algorithm. IET Renew Power Gener 2017;11(12):1517–26.
[4] Hasanien Hany M. An adaptive control strategy for low voltage ride through capability enhancement of grid-connected photovoltaic power plants. IEEE Trans Power Syst 2016;31(4):3230–7.
[5] Renewables 2018 Global status report, 2018. [Online]. Available: http://www.ren21.net/status-of-renewables/global-status-report/. [Accessed: 05-Jan-2019].
[6] Coester A, Hofkes MW, Papyrakis E. Economics of renewable energy expansion and security of supply: A dynamic simulation of the German electricity market. Appl Energy 2018;231:1268–84.
[7] Kim K, Park H, Kim H. Real options analysis for renewable energy investment decisions in developing countries. Renew Sustain Energy Rev 2017;75:918–26.
[8] Wang S, Tarroja B, Schell LS, Shaffer B, Samuelsen S. Prioritizing among the end uses of excess renewable energy for cost-effective greenhouse gas emission reductions. Appl Energy 2019;235:284–98.
[9] Hu H, Xie N, Fang D, Zhang X. The role of renewable energy consumption and commercial services trade in carbon dioxide reduction: Evidence from 25 developing countries. Appl Energy 2018;211:1229–44.
[10] Renewable Power Generation Costs in 2017, 2018. [Online]. Available: https://www.irena.org. [Accessed: 11-Nov-2018].
[11] The worlds biggest solar power plants, 2018. [Online]. Available: https://www.power-technology.com. [Accessed: 03-Jan-2019].
[12] Wang A, Xuan Y. A detailed study on loss processes in solar cells. Energy 2018;144:490–500.
[13] Khanna V, Das BK, Bisht D, Vandana, Singh PK. A three diode model for industrial solar cells and estimation of solar cell parameters using PSO algorithm. Renew Energy 2015;78:105–13.
[14] Nishioka K, Sakitani N, Uraoka Y, Fuyuki T. Analysis of multicrystalline silicon solar cells by modified 3-diode equivalent circuit model taking leakage current through periphery into consideration. Sol Energy Mater Sol Cells 2007;91(13):1222–7.
[15] Chaibi Y, Salhi M, El-jouni A, Essadki A. A new method to extract the equivalent circuit parameters of a photovoltaic panel. Sol Energy 2018;163:376–86.
[16] Şentürk A. New method for computing single diode model parameters of photovoltaic modules. Renew Energy 2018;128:30–6.
[17] Batzelis EI, Papathanassiou SA. A method for the analytical extraction of the single-diode PV model parameters. IEEE Trans Sustain Energy 2016;7(2):504–12.
[18] Ghani F, Duke M, Carson J. Numerical calculation of series and shunt resistances and diode quality factor of a photovoltaic cell using the Lambert W-function. Sol Energy 2013;91:422–31.
[19] Lun S, Wang S, Yang G, Guo T. A new explicit double-diode modeling method based on Lambert W-function for photovoltaic arrays. Sol Energy 2015;116:69–82.
[20] Khezzar R, Zereg M, Khezzar A. Modeling improvement of the four parameter model for photovoltaic modules. Sol Energy 2014;110:452–62.
[21] Di Piazza MC, Luna M, Petrone G, Spagnuolo G. Translation of the single-diode PV model parameters identified by using explicit formulas. IEEE J Photovoltaics 2017;7(4):1009–16.
[22] Celik AN, Acikgoz N. Modelling and experimental verification of the operating current of mono-crystalline photovoltaic modules using four- and five-parameter models. Appl Energy 2007;84(1):1–15.
[23] Bai J, Liu S, Hao Y, Zhang Z, Jiang M, Zhang Y. Development of a new compound method to extract the five parameters of PV modules. Energy Convers Manage 2014;79:294–303.
[24] Cuce E, Cuce PM, Karakas IH, Bali T. An accurate model for photovoltaic (PV) modules to determine electrical characteristics and thermodynamic performance parameters. Energy Convers Manage 2017;146:205–16.
[25] El Achouby H, Zaimi M, Ibral A, Assaid EM. New analytical approach for modelling effects of temperature and irradiance on physical parameters of photovoltaic solar module. Energy Convers Manage 2018;177:258–71.
[26] Toledo FJ, Blanes JM, Galiano V. Two-step linear least-squares method for photovoltaic single-diode model parameters extraction. IEEE Trans Ind Electron 2018;65(8):6301–8.
[27] Ishaque K, Salam Z, Taheri H. Simple, fast and accurate two-diode model for photovoltaic modules. Sol Energy Mater Sol Cells 2011;95(2):586–94.
[28] Et-torabi K, et al. Parameters estimation of the single and double diode photovoltaic models using a Gauss-Seidel algorithm and analytical method: A comparative study. Energy Convers Manage 2017;148:1041–54.
[29] Yahya-Khotbehsara A, Shahhoseini A. A fast modeling of the double-diode model for PV modules using combined analytical and numerical approach. Sol Energy 2018;162:403–9.
[30] Chatterjee A, Keyhani A, Kapoor D. Identification of photovoltaic source models. IEEE Trans Energy Convers 2011;26(3):883–9.
[31] Ayang A, et al. Maximum likelihood parameters estimation of single-diode model of photovoltaic generator. Renew Energy 2019;130:111–21.
[32] Cárdenas AA, Carrasco M, Mancilla-David F, Street A, Cárdenas R. Experimental parameter extraction in the single-diode photovoltaic model via a reduced-space search. IEEE Trans Ind Electron 2017;64(2):1468–76.
[33] Laudani A, Riganti Fulginei F, Salvini A. High performing extraction procedure for the one-diode model of a photovoltaic panel from experimental I-V curves by using reduced forms. Sol Energy 2014;103:316–26.
[34] Nunes HGG, Pombo JAN, Mariano SJPS, Calado MRA, Felippe de Souza JAM. A new high performance method for determining the parameters of PV cells and modules based on guaranteed convergence particle swarm optimization. Appl Energy 2018;211:774–91.
[35] Wu L, et al. Parameter extraction of photovoltaic models from measured I-V characteristics curves using a hybrid trust-region reflective algorithm. Appl Energy

2018;232:36–53.
[36] Abd Elaziz M, Oliva D. Parameter estimation of solar cells diode models by an improved opposition-based whale optimization algorithm. Energy Convers Manage 2018;171:1843–59.
[37] Oliva D, Abd El Aziz M, Ella Hassanien A. Parameter estimation of photovoltaic cells using an improved chaotic whale optimization algorithm. Appl Energy 2017;200:141–54.
[38] Xiong G, Zhang J, Shi D, He Y. Parameter extraction of solar photovoltaic models using an improved whale optimization algorithm. Energy Convers Manage 2018;174:388–405.
[39] Elazab OS, Hasanien HM, Elgendy MA, Abdeen AM. Parameters estimation of single- and multiple-diode photovoltaic model using whale optimisation algorithm. IET Renew Power Gener 2018;12(15):1755–61.
[40] Beigi AM, Maroosi A. Parameter identification for solar cells and module using a Hybrid Firefly and Pattern Search Algorithms. Sol Energy 2018;171:435–46.
[41] Kler D, Sharma P, Banerjee A, Rana KPS, Kumar V. PV cell and module efficient parameters estimation using Evaporation Rate based Water Cycle Algorithm. Swarm Evol Comput 2017;35:93–110.
[42] Abbassi R, Abbassi A, Heidari AA, Mirjalili S. An efficient salp swarm-inspired algorithm for parameters identification of photovoltaic cell models. Energy Convers Manage 2019;179:362–72.
[43] Yu K, Qu B, Yue C, Ge S, Chen X, Liang J. A performance-guided JAYA algorithm for parameters identification of photovoltaic cell and module. Appl Energy 2019;237:241–57.
[44] Askarzadeh A, Rezazadeh A. Parameter identification for solar cell models using harmony search-based algorithms. Sol Energy 2012;86(11):3241–9.
[45] Alam DF, Yousri DA, Eteiba MB. Flower Pollination Algorithm based solar PV parameter estimation. Energy Convers Manage 2015;101:410–22.
[46] Yu K, Liang JJ, Qu BY, Cheng Z, Wang H. Multiple learning backtracking search algorithm for estimating parameters of photovoltaic models. Appl Energy 2018;226:408–22.
[47] Chen X, Xu B, Mei C, Ding Y, Li K. Teaching–learning–based artificial bee colony for solar photovoltaic parameter estimation. Appl Energy 2018;212:1578–88.
[48] Chin VJ, Salam Z, Ishaque K. An accurate modelling of the two-diode model of PV module using a hybrid solution based on differential evolution. Energy Convers Manage 2016;124:42–50.
[49] Ishaque K, Salam Z, Mekhilef S, Shamsudin A. Parameter extraction of solar photovoltaic modules using penalty-based differential evolution. Appl Energy 2012;99:297–308.
[50] Chellaswamy C, Ramesh R. Parameter extraction of solar cell models based on adaptive differential evolution algorithm. Renew Energy 2016;97:823–37.
[51] Biswas PP, Suganthan PN, Wu G, Amaratunga GAJ. Parameter estimation of solar cells using datasheet information with the application of an adaptive differential evolution algorithm. Renew Energy 2019;132:425–38.
[52] Hasanien HM. Shuffled Frog Leaping Algorithm for Photovoltaic Model Identification. IEEE Trans Sustain Energy 2015;6(2):509–15.
[53] Subudhi B, Pradhan R. Bacterial foraging optimization approach to parameter extraction of a photovoltaic module. IEEE Trans Sustain Energy 2018;9(1):381–9.
[54] Allam D, Yousri DA, Eteiba MB. Parameters extraction of the three diode model for the multi-crystalline solar cell/module using Moth-Flame Optimization Algorithm. Energy Convers Manage 2016;123:535–48.
[55] Gomes GF, da Cunha SS, Ancelotti AC. A sunflower optimization (SFO) algorithm applied to damage identification on laminated composite plates. Eng Comput 2018.
[56] Briggs WR. How do sunflowers follow the Sun—and to what end? Science (80-.) 2016;353(6299):541 LP-542.
[57] Kyocera, KC200GT Kyocera PV module datasheet, 2018. [Online]. Available: http://www.kyocera.com.sg/products/solar/pdf/kc200gt.pdf. [Accessed: 01-Dec-2018].
[58] Solarex, MSX-60 PV module Solarex datasheet, 2018. [Online]. Available: http://www.solarelectricsupply.com/solar-panels/solarex/solarex-msx-60-w-junction-box. [Accessed: 01-Dec-2018].
[59] CS6K-280M canadiansolar PV module datasheet. [Online]. Available: https://www.canadiansolar.com/downloads/datasheets/v5.5/Canadian_Solar-Datasheets-CS6K-M-v5.52en.pdf. [Accessed: 01-Dec-2018].
[60] Top 10 module suppliers. [Online]. Available: https://www.pv-tech.org/editors-blog/top-10-module-suppliers-in-2017. [Accessed: 01-Dec-2018].
[61] Release 2016b, “MATLAB,” The Math Works press, Sep., 2016 [accessed 13 Sept., 2017].
[62] Villalva MG, Gazoli JR, Filho ER. Comprehensive approach to modeling and simulation of photovoltaic arrays. IEEE Trans Power Electron 2009;24(5):1198–208.
[63] Hasanien Hany M. Whale optimisation algorithm for automatic generation control of interconnected modern power systems including renewable energy sources. IET Gener Transm Distrib 2018;12(3):607–14.